Science of the Total Environment 952 (2024) 175753

Contents lists available at ScienceDirect

Science of the Total Environment

journal homepage: www.elsevier.com/locate/scitotenv

The linkage between functional traits and drone-derived phenology of 74 Northern Hemisphere tree species

Simon Kloos [a], Marvin Lüpke [a], Nicole Estrella [a], Wael Ghada [a], Jens Kattge [b,c], Solveig Franziska Bucher [c,d], Allan Buras [e], Annette Menzel [a,f,*]

[a] TUM School of Life Sciences, Ecoclimatology, Technical University of Munich, Hans-Carl-von-Carlowitz-Platz 2, 85354 Freising, Germany
[b] Max Planck Institute for Biogeochemistry, Hans-Knöll-Straße 10, 07745 Jena, Germany
[c] German Centre for Integrative Biodiversity Research (iDiv) Halle-Jena-Leipzig, Puschstraße 4, 04103 Leipzig, Germany
[d] Institute of Ecology and Evolution, Plant Biodiversity Group, Friedrich Schiller University Jena, Philosophenweg 16, 07743 Jena, Germany
[e] TUM School of Life Sciences, Land Surface-Atmosphere Interactions, Technical University of Munich, Hans-Carl-von-Carlowitz-Platz 2, 85354 Freising, Germany
[f] Institute for Advanced Study, Technical University of Munich, Lichtenbergstraße 2a, 85748 Garching, Germany

HIGHLIGHTS

- UAV-derived phenology for 3099 individuals and 74 Northern Hemispheric tree species
- High agreement with in-situ leaf unfolding and discoloration data (R^2 = 0.49/0.79)
- Variations in the length of the growing season of up to two months
- Functional traits explaining interspecific phenological differences by up to 55 %

GRAPHICAL ABSTRACT

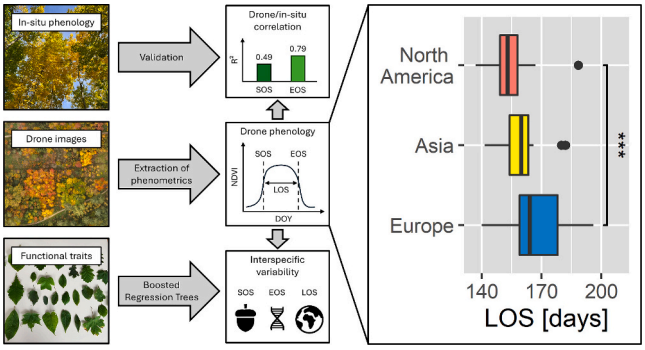

ARTICLE INFO

Editor: Manuel Esteban Lucas-Borja

Keywords:
UAV
Leaf unfolding
Senescence
Growing season
Phenological variability
Plant traits

ABSTRACT

Tree phenology is a major component of the global carbon and water cycle, serving as a fingerprint of climate change, and exhibiting significant variability both within and between species. In the emerging field of drone monitoring, it remains unclear whether this phenological variability can be effectively captured across numerous tree species. Additionally, the drivers behind interspecific variations in the phenology of deciduous trees are poorly understood, although they may be linked to plant functional traits. In this study, we derived the start of season (SOS), end of season (EOS), and length of season (LOS) for 3099 individuals from 74 deciduous tree species of the Northern Hemisphere at a unique study site in southeast Germany using drone imagery. We validated these phenological metrics with in-situ data and analyzed the interspecific variability in terms of plant functional traits. The drone-derived SOS and EOS showed high agreement with ground observations of leaf unfolding (R^2 = 0.49) and leaf discoloration (R^2 = 0.79), indicating that this methodology robustly captures

* Corresponding author at: TUM School of Life Sciences, Ecoclimatology, Technical University of Munich, Hans-Carl-von-Carlowitz-Platz 2, 85354 Freising, Germany.
E-mail addresses: simon.kloos@tum.de (S. Kloos), marvin.luepke@tum.de (M. Lüpke), estrella@tum.de (N. Estrella), jkattge@bgc-jena.mpg.de (J. Kattge), solveig.franziska.bucher@uni-jena.de (S.F. Bucher), allan.buras@tum.de (A. Buras), annette.menzel@tum.de (A. Menzel).

https://doi.org/10.1016/j.scitotenv.2024.175753
Received 29 May 2024; Received in revised form 2 August 2024; Accepted 22 August 2024
Available online 30 August 2024

phenology at the individual level with low temporal and human effort. Both intra- and interspecific phenological variability were high in spring and autumn, leading to differences in the LOS of up to two months under almost identical environmental conditions. Functional traits such as seed dry mass, chromosome number, and continent of origin played significant roles in explaining interspecific phenological differences in SOS, EOS, and LOS, respectively. In total, 55 %, 39 %, and 45 % of interspecific variation in SOS, EOS, and LOS could be explained by the Boosted Regression Tree (BRT) models based on functional traits. Our findings encourage new research avenues in tree phenology and advance our understanding of the growth strategies of key tree species in the Northern Hemisphere.

1. Introduction

Plant phenology is an important indicator of the ecological impacts of climate change (Cleland et al., 2007; Menzel et al., 2020; Piao et al., 2019) and influences essential functions of terrestrial ecosystems such as photosynthetic activity (Keenan et al., 2014; Piao et al., 2007; Tang et al., 2016) or evapotranspiration (Gaertner et al., 2019; Kim et al., 2018). Spring phenology is primarily controlled by temperature (Ettinger et al., 2020; Flynn and Wolkovich, 2018; Menzel et al., 2006) and shows mostly advancing trends in the northern hemisphere due to global warming in recent decades (Melaas et al., 2018; Menzel et al., 2020; Vitasse et al., 2022). In contrast, autumn phenology is slightly delayed with global warming, but the responses are much more heterogeneous (Garonna et al., 2016; Piao et al., 2019) and the drivers are still not fully understood (Gill et al., 2015; Kloos et al., 2024; Lu and Keenan, 2022; Zohner et al., 2023). Offsetting the onset dates of spring and autumn phenology against each other, the growing season length (phenological season; Körner et al., 2023) can be obtained.

In analyses of both trends and drivers for spring and autumn phenology, as well as the resulting growing season length, phenological variability is a frequently underestimated factor. For example, in twelve years of phenological observations in a North American forest (16 canopy species), roughly six weeks of interspecific difference in budburst and almost three weeks of difference in leaf coloration were observed (Richardson and O'Keefe, 2009). Two years of in-situ budburst observations in six deciduous tree species and a total of 825 individuals in a European woodland showed species-specific differences of up to 42 days (Cole and Sheldon, 2017). On the other hand, phenological variability can also be observed within tree species: Budburst, for example, has been observed to vary between individuals of *Quercus petraea* by up to 26 days and the onset of senescence by up to 51 days between individuals of *Betula pendula* at the same location. In general the autumn phenology seems to exhibit a higher intraspecific variability (Capdevielle-Vargas et al., 2015; Delpierre et al., 2017; Marchand et al., 2020). The age and height of the trees play an important role in observing spring and autumn phenology for smaller and subcanopy individuals in a stand (Augspurger and Bartlett, 2003; Gressler et al., 2015; Osada and Hiura, 2019; Uphus et al., 2021).

For trend- and driver-analyses in plant phenology, these forms of variability primarily translate into unexplained variance. From an ecological perspective, phenological variability may also constitute a major factor for resilience against extremes, e.g., late spring frost damage (Diez et al., 2012). Consequently, this inter-and intraspecific variability is of great interest. The correlation of interspecific variation of phenology to biotic factors (and especially plant functional traits) could be used to get a better understanding of climate-resilient forest species and to open avenues to extrapolation of single species results. In the last decades, many studies have demonstrated the significance of functional traits for the onset dates of certain phenological phases of different, however mostly herbaceous species: In previous studies, for example, plant height (e.g., Horbach et al., 2023; Sporbert et al., 2022; Sun and Frelich, 2011), seed dry mass (e.g., Bolmgren and Cowan, 2008; Du and Qi, 2010; Segrestin et al., 2020), leaf area (Liu ZhiGuo et al., 2011; Sun et al., 2006) and leaf thickness (Craine et al., 2012; Horbach et al., 2023), leaf area per leaf dry mass (specific leaf area, SLA; Bucher et al., 2018; Bucher and Römermann, 2021; Horbach et al., 2023; Sporbert et al., 2022), leaf dry mass per leaf fresh mass (leaf dry matter content, LDMC; Horbach et al., 2023; Sporbert et al., 2022) and chemical properties of the leaf such as phosphorus (P; Bucher et al., 2018), carbon (C; Bucher and Römermann, 2021; Sporbert et al., 2022) or nitrogen (N; Bucher et al., 2018; Craine et al., 2012; Sporbert et al., 2022) content were associated with different phenological phases. Less recognized traits in connection with plant phenology are the rooting depth (Dorji et al., 2013) and the diameter of the spring/xylem vessels (Lechowicz, 1984; Panchen et al., 2014). Finally, Zohner and Renner (2017) revealed that the native region of a plant also has an influence on spring and autumn phenology and can therefore determine the length of the growing season.

However, to date, the link between onset dates of phenological phases, especially the beginning and end of the growing season, and functional traits has hardly been studied for deciduous tree species. On the one hand, this is because there are barely any sites with an adequate number of different tree species with mature individuals. On the other hand, the in-situ observation of different phenological phases and functional traits on the individual level is extremely time-consuming and resource-intensive. A relatively new approach for solving the phenological monitoring problem is the derivation of plant phenology via unmanned aerial vehicles (UAV): Various phenological metrics (especially SOS and EOS) can be monitored via drone images and the resulting spectral indices (e.g., Dandois and Ellis, 2013; Klosterman and Richardson, 2017; Kleinsmann et al., 2023). The main advantage of this method is that, compared to satellite remote sensing, the spatial resolution is much higher, and thus analyses at the individual level are possible. At the same time, a larger area and more individuals can be covered than with in-situ observations. Studies specifically analyzing deciduous tree phenology have received ambiguous but acceptable results when comparing drone-derived phenology and the phenology deduced from other data sources such as in-situ observations or satellite remote sensing (Berra et al., 2019; Berra and Gaulton, 2021). Only a few studies exist which evaluate the phenology of several deciduous tree species via drone: Wu et al. (2021) combined PlanetScope and drone data for the autumn phenology of eleven canopy tree species in northeast China and found high agreement with phenocams, while Fawcett et al. (2021) showed understory effects in the drone-derived spring phenology of a heterogeneous ecosystem in the UK. These understory effects might also explain poor drone coverage of inter- and intraspecific spring phenological variability in a Japanese study (19 deciduous broadleaved species; Budianti et al., 2021), whereas a follow-up study with 17 species showed partly significant correlation between drone and ground-observed phenometrics (Budianti et al., 2022).

However, several research gaps appear: First, there are (to our knowledge) no analyses in the still young research field of drone monitoring that have tested whether realistic phenological data sets can be generated for a large number (>20) of deciduous tree species using a drone flight series. Second, there are hardly any studies available that systematically analyze the inter- and intraspecific variability of spring and autumn phenology and the length of the growing season for a large number of deciduous tree species at one site. As a result, there is little knowledge about the relationship or influence of functional traits on different phenological phases and metrics, such as SOS, EOS, or LOS,

especially for deciduous tree species. Applying a year-round drone monitoring of 74 deciduous tree species from the Northern Hemisphere with a total of 3099 individuals at a unique study site in southeast Germany, our study asks the following research questions:

1. Can the spring and autumn phenology, along with the resulting length of the growing season, of a diverse array of deciduous tree species at a single site be accurately determined using drone data and a universal method applicable to all species?
2. To what extent do the determined phenological metrics (SOS, EOS, LOS) vary between and within the individual tree species under almost identical environmental conditions?
3. Can the observed interspecific phenological variability be explained by functional traits of the respective tree species, and if so, which traits play a dominant role?

We hypothesize therefore that the phenological metrics SOS, EOS, and LOS for a diverse array of deciduous tree species at a single site can be accurately determined using drone data and a universal method applicable to all species, and the observed interspecific phenological variability can be partly explained by plant functional traits.

2. Materials and methods

2.1. Study site

The study was conducted in the "Weltwald Freising" (World Forest), which is located in southeastern Germany (48°24′50″N, 11°40′00″E; 462 to 508 m a.s.l.; State Office for Digitization, Broadband and Surveying, 2023; Fig. 1). The area of the forest is about 100 ha and >400 tree and shrub species of the Northern Hemisphere have been planted there since 1987 (Rudolf, 2023). The arboretum is divided according to the continental origin of the tree and shrub species. Species are planted in plots, each containing from a few single individuals to nearly 200 specimens of the respective species. Only deciduous tree species were selected for the analysis since their phenological phases are easier and more robust to detect using drone data than for evergreen species.

Most of the soils in the study area are deep, mixed substrates of Tertiary (gravels, sands) and Quaternary (loess loam) sediments, which have a high nutrient availability and water retention capacity. The regional climate is subatlantic to subcontinental, the mean annual temperature is 9.4 °C and the mean annual precipitation is 736 mm (2001–2020; DWD, 2024; Rudolf, 2023). In the observation year 2022, the mean temperature in the study area was 9.6 °C, and the annual precipitation total was 829 mm (for further details see Fig. S1; data provided by the Bavarian State Institute of Forestry). The climate in various parts of the forest should be homogeneous within the study area and between the individual continental areas due to the small differences in altitude (see Fig. S2).

2.2. Data

2.2.1. Drone imagery

To observe the phenological development at the study site, flights with a Phantom 4 multispectral UAV (DJI, Nanshan, Shenzhen, China) at 100 m a.g.l. flight height with a ground sampling distance of 5–8 cm were planned twice per week in spring and autumn and once per week in summer in 2022. Due to limited optimal flight conditions we achieved 27 flights in total. Images were taken once per second at the red (650 nm ± 16 nm), near-infrared (NIR; 840 nm ± 26 nm), and RGB cameras at a 2 MP resolution in NADIR position. The drone used an integrated dual-band high precision Real Time Kinematic (RTK) GPS with Networked

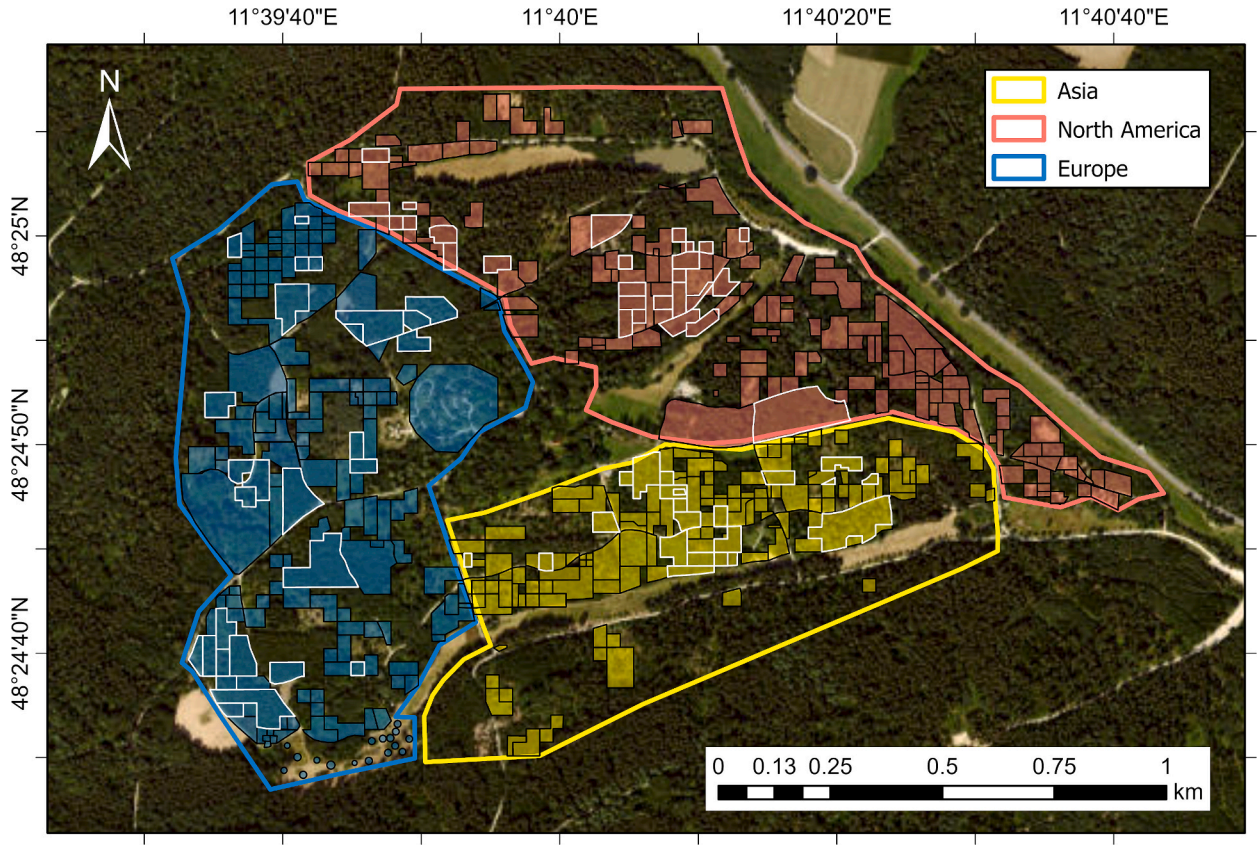

Fig. 1. Map of Weltwald Freising. The areas marked in color represent the individual tree species plots, whereby the plots framed in white are the analyzed tree species plots within this study (for the selection criteria see Section 2.3.1; yellow: Asia; blue: Europe; red: North America; background map: Maxar, Microsoft; polygon data: Bavarian State Forestry, 2022).

Transport of RTCM via Internet Protocol (NTRIP) network service to get a repeatable position accuracy (up to 0.1 m vertical and horizontal precision according to the manufacturer manual). To enhance accuracy further, at least five measured ground control points were placed in each flight area. The flight grid was set up with a frontal and lateral overlap of 85 %. The orientation of the grid was set by the flight software automatically according to sun direction, sun angle, and date to avoid disturbance from sunlight on the camera sensor. This was important since flights were also conducted in early spring and late autumn with typically lower sun angles compared to summer months.

All settings were optimized for the highest flight speed and therefore to achieve largest coverage and avoid strong shadow movement. Optimal drone orthomosaics are usually generated under overcast and calm (no wind) conditions, as images with even illumination do not have any shadows and canopies are not blurred due to movement. Since such conditions are rare, flight days with uniform clear skies or overcast conditions and low wind speeds were targeted. The 8 flights were typically operated around noon with highest sun angle, in order to avoid long shadows. One flight lasted from 11 to 14 min and covered an area from 7.9 to 8.9 ha. The exact flight dates are listed in Table S1.

Before each flight, a picture of a calibration reflectance panel (AgEagle Aerial Systems Inc., Wichita, Kansas, USA) was taken since this was a requirement for the processing software PIX4d to calculate reflectance values for both spectral channels. The drone images were processed in PIX4d mapper Version 4.75 (Pix4D, Prilly, Switzerland) to generate RGB orthomosaics, Normalized Difference Vegetation Index (NDVI) maps, a digital terrain model (DTM), a digital surface model (DSM), and 3D point clouds. A custom configuration was used to process the images (Table S2) since the standard setting worked insufficiently with the drone cameras. The output resolution for all images was set to 10 cm, except the DTM with 1 m resolution.

2.2.2. In-situ observations

For validation purposes, the phenology of selected tree species was observed from the ground in spring and autumn 2022. In spring, 45 of the 74 tree species observed with the drone were monitored from in-situ (Table S3). From the end of March to the end of May, the average phenological phase of each tree species was recorded plot-wise twice a week based on a categorical scale (Vitasse et al., 2013):

- 0: buds closed (no bud activity)
- 1: budburst (buds are open and leaves are partially visible)
- 2: leaf emergence (leaves fully emerged from the buds but are still folded, crinkled or pendant)
- 3: leaf unfolding (for each tree at least one leaf is fully unfolded)

For the validation of the drone-derived SOS, the date on which phase 3 was observed for the first time from the ground was selected for each tree species.

In autumn, 27 of the 74 species monitored with the drone were additionally observed from the ground (Table S3). Between mid-September and early December, the degree of leaf discoloration and leaf fall of the respective tree species was estimated plot-wise twice a week in 10 % steps. For leaf discoloration, this included fallen leaves on the ground in the estimates. Therefore, the number of leaves hanging on the tree and immediately below was analyzed as a total and the proportion of discolored leaves was estimated accordingly. For validation with the drone-based EOS, the degree of leaf discoloration was finally interpolated at a daily time resolution and the date on which the proportion of discolored leaves for the first time reached at least 50 % was determined as ground-truth EOS. To validate the drone-derived phenology with the in-situ data, a simple linear regression was calculated between the two data sets, and the associated coefficient of determination and p-value were defined. The mean difference between the two onset dates and the percentage of species exhibiting at maximum five days of deviation was used as a further evaluation measure for spring and autumn. Not all drone-monitored species were validated on the ground due to the extensive study area, which demanded significant time and personnel resources for on-site observations.

2.2.3. Functional traits

To explain differences in the interspecific variability of phenology in the study area as derived from drone flights, 13 functional traits of the tree species (Table 1) were included in the analysis, selected from an initial set of 23 numerical traits (Table S4). The age of the tree species was determined from planting dates provided by the Bavarian State Forestry (2022), whereas the mean tree height and crown area of each tree species were derived from the drone data (via crown extraction and selection, see 2.3.1). The number of chromosomes was determined for the individual tree species using the CCBD (Chromosome Counts Database; Rice et al., 2015) whereby the respective median was assigned to each species. In addition to the numerical traits, the continent of origin was included as a categorical trait variable for each tree species.

The other numerical traits were extracted from the TRY plant trait database (Kattge et al., 2020): Originally, a trait matrix with the trait measurements for all available species from the TRY database was created. The data were transformed into a normal distribution and then z-transformed. The gaps in the matrix were then filled using the Bayesian hierarchical probabilistic matrix factorization (BHPMF) gap-filling algorithm (Schrodt et al., 2015), which is based on probabilistic matrix factorization (PMF) and the taxonomic hierarchy of the plant kingdom. Subsequently, the matrix values were transformed back, and finally outliers were removed based on the z-transformation.

For 70 study species (*Alnus rugosa*, *Carya tomentosa*, *Populus trichocarpa*, and *Pterocarya fraxinifolia* are not included in TRY), a mean value was then calculated for each trait and species from the individual values in the TRY data set. Based on the "stable species hierarchy" hypothesis, it can be assumed that although these mean values do not necessarily correspond to the values for the study area in absolute terms, the hierarchical arrangement of values between species should remain approximately the same (e.g., Kazakou et al., 2014; Cordlandwehr et al., 2013; Violle et al., 2015).

The final selection of numerical traits (Table 1) for the Boosted Regression Trees (BRT) analysis (Section 2.3.3) was based on two criteria: In the first step, all traits were selected for which a connection to plant phenology had already been established in the existing literature (see Table 1). In the second step, additional traits were included which showed a statistically significant correlation with the phenological metrics determined from the drone data (Table S4; Section 2.3.2).

2.2.4. Climate distances

To represent the climatic origin of each tree species, we combined species-specific distribution maps with so-called climate distances (Buras and Menzel, 2019). These climate distances represent conflated Manhattan distances of the 30-year climatology of 11 climate variables (e.g. growing season length, climatic water balance of the driest month, for details see Supplementary Table S2 in Buras and Menzel, 2019) representing the period 1961–1990. Climate distances were based on CRU TS (v 4.01; Harris et al., 2020) temperature data and GPCC precipitation data (Schneider et al., 2011) which are available at monthly temporal and 0.5° spatial resolution. To represent the climatic distance of each species under investigation, we extracted the climate distances to the grid-cell representative of our study site (48.25°N, 11.25°E) for all terrestrial grid cells on Earth. Thus, the extracted values represent a measure of the dissimilarity of each grid cells' climate to the climate in our study site. Further details on the derivation of climate distances are specified in Buras and Menzel (2019).

To assign a climate distance for each tree species, the distribution area of the respective species was determined. For European species, the distribution in terms of chorological maps (Caudullo et al., 2017) and relative probability of presence (RPP; de Rigo et al., 2016) were

Table 1
Functional traits used for analysis of interspecific variability in phenology. The table indicates their units, lists studies that have linked the relationship of the respective trait to a plant phenological phase, and summarizes the respective type of correlation. The table distinguishes between tree species (bold) and non-tree species (normal font) studies.

Plant trait	Unit	Link to plant phenology	Correlation between trait and phenological onset date
Tree (plant) height	m	**Horbach et al., 2023**; Sporbert et al., 2022; Liu et al., 2021; Segrestin et al., 2020; **König et al., 2018**; Lauterbach et al., 2013; Sun and Frelich, 2011; **Du and Qi, 2010**; **Bolmgren and Cowan, 2008**; Vile et al., 2006; Louault et al., 2005	Positive (all phenophases, especially flowering)
Leaf area	mm^2	Sporbert et al., 2022; Segrestin et al., 2020; Craine et al., 2012; **Liu ZhiGuo et al., 2011**; **Sun et al., 2006**	Positive (leaf unfolding) and negative (flowering, fruiting, senescence)
Leaf thickness	mm	**Horbach et al., 2023**; Craine et al., 2012	Negative (leaf unfolding and flowering)
Leaf area per leaf dry mass (SLA)	mm^2 mg^{-1}	**Horbach et al., 2023**; Sporbert et al., 2022; Bucher and Römermann, 2021; Bucher et al., 2018; **König et al., 2018**; Lauterbach et al., 2013; Sun and Frelich, 2011; Vile et al., 2006	Positive (fruiting) and negative (leaf unfolding)
Leaf dry mass per leaf fresh mass (LDMC)	$g\ g^{-1}$	**Horbach et al., 2023**; Sporbert et al., 2022; Bucher and Römermann, 2021; **König et al., 2018**	Positive (leaf unfolding) and negative (flowering)
Seed dry mass	mg	Sporbert et al., 2022; Liu et al., 2021; Segrestin et al., 2020; Craine et al., 2012; **Du and Qi, 2010**; **Bolmgren and Cowan, 2008**; Vile et al., 2006; Louault et al., 2005	Negative (flowering)
Leaf N content per leaf dry mass	$mg\ g^{-1}$	Sporbert et al., 2022; Bucher and Römermann, 2021; Segrestin et al., 2020; Bucher et al., 2018; Craine et al., 2012	Negative (leaf unfolding, flowering, fruiting)
Leaf C content per leaf dry mass	$mg\ g^{-1}$	Sporbert et al., 2022; Bucher and Römermann, 2021; Craine et al., 2012	Positive (leaf unfolding, fruiting, senescence)
Leaf P content per leaf dry mass	$mg\ g^{-1}$	Segrestin et al., 2020; Bucher et al., 2018	Negative (flowering)
Root rooting depth	m	Dorji et al., 2013	Positive (flowering)
Stem conduit diameter	micro m	**Lechowicz, 1984**; **Panchen et al., 2014**	Positive (leaf unfolding)
Chromosome number	n	Included due to high correlation values with extracted phenological metrics (2.3.2; Table S4)	Negative (senescence)
Fine root length per fine root dry mass (specific root length, SRL)	$cm\ g^{-1}$	Included due to high correlation values with extracted phenological metrics (2.3.2; Table S4)	Positive (leaf unfolding)

obtained from the website of the Joint Research Centre of the European Commission. Synanthropic occurrences were excluded to keep the focus on the natural distribution of the species. Equally, we excluded fragmented isolated occurrences to avoid including entire grid cells for the sake of only a few observations. For all other species, the GBIF (Global Biodiversity Information Facility, 2021) occurrence data were used. We limited our research to tree-species observations after 1900 and excluded species that did not occur in at least 100 grid cells considering a global resolution of 0.5° x 0.5°. For the resulting 60 (of 74) individual species distributions, we extracted all climate distances for further processing. To avoid the effect of a large distribution area, we identified for each tree species the regions in the chorological map where the climate distance to the study area was within the lower 20 % quantile. Within these regions, we calculated the median of climate distances to the study area.

2.3. Methods

2.3.1. Extraction and selection of tree crowns

To extract phenology on an individual tree level, single tree canopies needed to be identified from the drone images. As input for the tree detection algorithms a canopy height model (CHM) was calculated from the difference between the DSM and the DTM. DTMs were constructed from the end of March (22nd and 28th) drone images, when all deciduous trees had no leaves, and the ground was clearly visible. DSM was obtained from drone images at the end of July (27th) when all canopies were fully developed.

Treetops were detected by a variable window filter (Popescu and Wynne, 2004) using the *vwf* function in the R (R Core Team, 2022) package *ForestTools* (v.1.0.1; Plowright and Roussel, 2023). The algorithm detects local maxima, which correspond to a treetop, via a specific window filter size in the CHM. The window size was set by a height-dependent function, starting from 3 m to 8 m CHM height with a constant value of 1, growing windows with a linear function (height * 0.06 + 0.52) from 8 to 35 m CHM height and a final constant of 2.62 above a CHM height of 35 m. The function was derived by comparing different functions against a manually derived treetop map from a small subset area of the Weltwald from the CHM and the orthomosaic. All treetops below 5 m were ignored since these mostly included shrubs and/or saplings. In a further step, unrealistic and falsely detected treetops were removed, and missing treetops were added by comparing the tops with multiple orthomosaics from spring, summer, and autumn.

Crowns were segmented from the filtered treetops with the algorithm by Dalponte and Coomes (2016) using the R (R Core Team, 2022) package *lidR* (v3.1.0; Roussel et al., 2023; Roussel et al., 2020). The algorithm used a height threshold of 5 m, a growing threshold 1 of 0.35, a growing threshold 2 of 0.55, and a maximum amount of 90 pixels for the crown diameter of a detected tree.

After the extraction of the tree crowns for the study area, the canopy area (in m^2) was calculated for all crowns. All individuals with a canopy area $< 3\ m^2$ were removed from the analysis to avoid tree crowns with a low pixel count. Within each plot, tree crowns were manually filtered, removing "non-circular" crowns (incorrectly determined by the algorithm, significantly longer than wide) from the final dataset. In addition, only crowns that were located within the planted plots and species (derived from Bavarian State Forestry, 2022) with a minimum number of five individuals within the plot were included in the analyses to ensure a higher representativeness of the results. In the last step, 10 cm (one pixel) reverse buffers were calculated around each tree crown to avoid overlaps and mixed pixels from two crowns. After the selection process, 74 tree species (Table S3) and 3099 individuals were included in the final analysis.

2.3.2. Extraction of phenological metrics

The extraction of the phenological metrics for the single trees was done in R (R Core Team, 2022) with the *phenex* package (v.1.4-5; Lange

and Doktor, 2022). In the first step, a raster stack of all 27 NDVI images of the year was created. Subsequently, we computed the median of the NDVI pixels within each of the respective tree crowns for each of the 27 scenes. A double logistic function was then fitted (Fischer, 1994) for each tree crown using the non-corrected 27 median NDVI values. To determine individual SOS and EOS dates from these fitted NDVI curves, percentage thresholds were set between the lowest, early-season (i.e., before peak-season NDVI) and highest NDVI value (SOS) and the highest and lowest, late-season NDVI (EOS) in the time series ("local" threshold). The SOS/EOS dates were then defined on the day when NDVI first exceeded or fell below these thresholds. Each threshold was tested in 10 % increments and the SOS/EOS results were compared to the observed in-situ data. The best validation results were obtained with a threshold of 0.5 for SOS and 0.7 for EOS. These phenological metrics were then used for all further analyses (for illustration, see Fig. S3). Finally, the length of the growing season (LOS) was calculated by subtracting SOS from EOS for each tree crown. To analyze differences in tree species phenology with respect to the continent of origin, a two-sided Wilcoxon test was calculated between the respective continent groups.

2.3.3. Boosted regression trees (BRT)

To explain the interspecific variability of SOS, EOS, and LOS in the study area by traits (2.2.3), a BRT analysis was conducted. BRTs are derived from Random Forests, distinguished by their use of a different learning procedure called Boosting. They have the advantage that predictor variables of any type (numeric, binary, categorical) can be used and that they are relatively insensitive to outliers and collinearity, which means that no variance inflation has to be calculated in advance (Elith et al., 2008; Sporbert et al., 2022). We altogether computed three BRTs, i.e. each one to model the variance of the tree species median SOS/EOS/LOS. As predictor variables we used 1) the 13 selected numerical traits (Table 1), 2) the continent of origin of the tree species as a categorical variable, and 3) the climatic distance calculated in each case (Section 2.2.4). The models were set up in R (R Core Team, 2022) using the package *dismo* (v1.3-14; Hijmans et al., 2023). We used a Gaussian error distribution, a tree complexity of 1, a learning rate of 0.003, and a bag fraction of 0.5 for all models. Finally, partial dependency plots and the relative importance (%) of all predictor variables in the models were calculated. To evaluate the model performance, we used cross-validation (cv) correlation and predicted (BRT) vs. observed (drone-derived) SOS, EOS, and LOS plots (see Figs. S4–6).

3. Results

3.1. Validation of drone phenology

When comparing the ground observations (first leaf unfolding) and the drone-derived spring phenology (SOS, local threshold: 0.5) for the individual tree species, a good agreement of the dates was found ($R^2 = 0.49$; $p < 0.001$; Fig. 2). 53 % of the observed tree species had an in-situ/drone SOS difference of at most five days and the mean difference between drone-derived and in-situ SOS was 5.6 days. For early leaf-unfolding species, the drone-derived SOS tended to be recorded later than the observed leaf emergence, while later sprouting species had the tendency to be assigned with earlier SOS values in comparison to the in-situ data. Validation differences between the individual continents of origin could not be determined, although North American species tended to leaf out later compared to the other continents.

When comparing the autumn phenology data, even higher agreement between the drone EOS (local threshold: 0.7) and the ground observations (50 % leaf discoloration) was observed than in spring ($R^2 = 0.79$; $p < 0.001$; Fig. 3). 93 % of the data points were within the 5-day deviation between drone-derived and observed autumn phenology and the mean difference between drone and in-situ EOS was 2.8 days. No differences were found within the validation in the distinction between

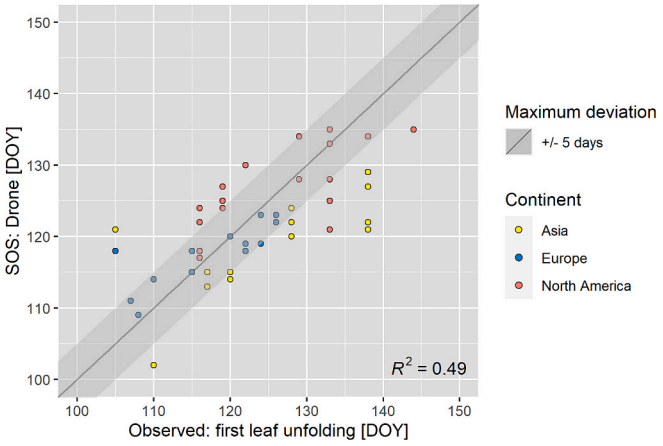

Fig. 2. Scatterplot of the observed first leaf unfolding, and the calibrated SOS determined by the drone images for the respective tree species. The observed tree species are color-coded according to the continent of origin (yellow: Asia; blue: Europe; red: North America). The dark gray line in the plot represents the area where the in-situ data and the drone data for spring phenology match perfectly. The dark gray area marks a maximum deviation of five days between in-situ and drone phenology (inside: 53 % of the observed tree species). The coefficient of determination is shown at the bottom right of the plot.

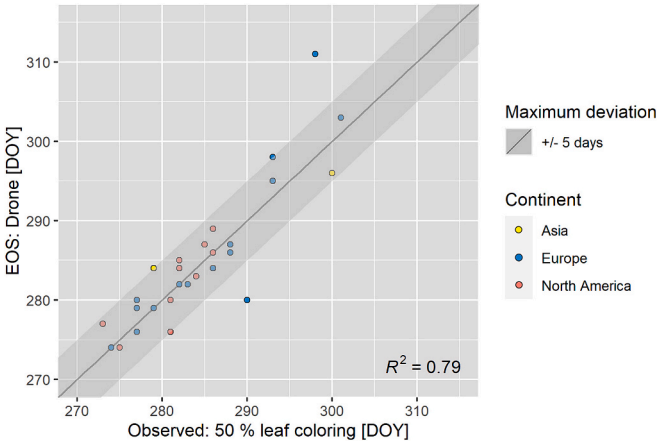

Fig. 3. Scatterplot between the observed 50 % leaf coloring, and the calibrated EOS determined by the drone images for the respective tree species. The observed tree species are color-coded according to the continent of origin (yellow: Asia; blue: Europe; red: North America). The dark gray line in the plot represents the area where the in-situ data and the drone data for autumn phenology match perfectly. The dark gray area marks a maximum deviation of five days between in-situ and drone phenology (inside: 93 % of the observed tree species). The coefficient of determination is shown at the bottom right of the plot.

early and late senescent species or in the continent of origin, whereas North American species were more likely to be early senescing species.

3.2. Tree phenology

The spring phenology (SOS) of the 74 tree species observed in the study area in 2022 ranged from the end of March to the end of May, with a difference of 41 days between the median of the first (*Prunus padus*; 4th of April) and the last leaf-unfolding species (*Carya tomentosa*; 15th of May; Fig. 4). In addition, it should be noted that there were a few species (*Prunus padus*, *Larix gemlinii* var. *principis-rupprechtii*, *Larix decidua* var. *polonica*) that unfolded their leaves/needles much earlier (6–14 days median difference) than the vast majority. Remarkable differences in SOS were also observed within species (*Fraxinus pennsylvanica* with an

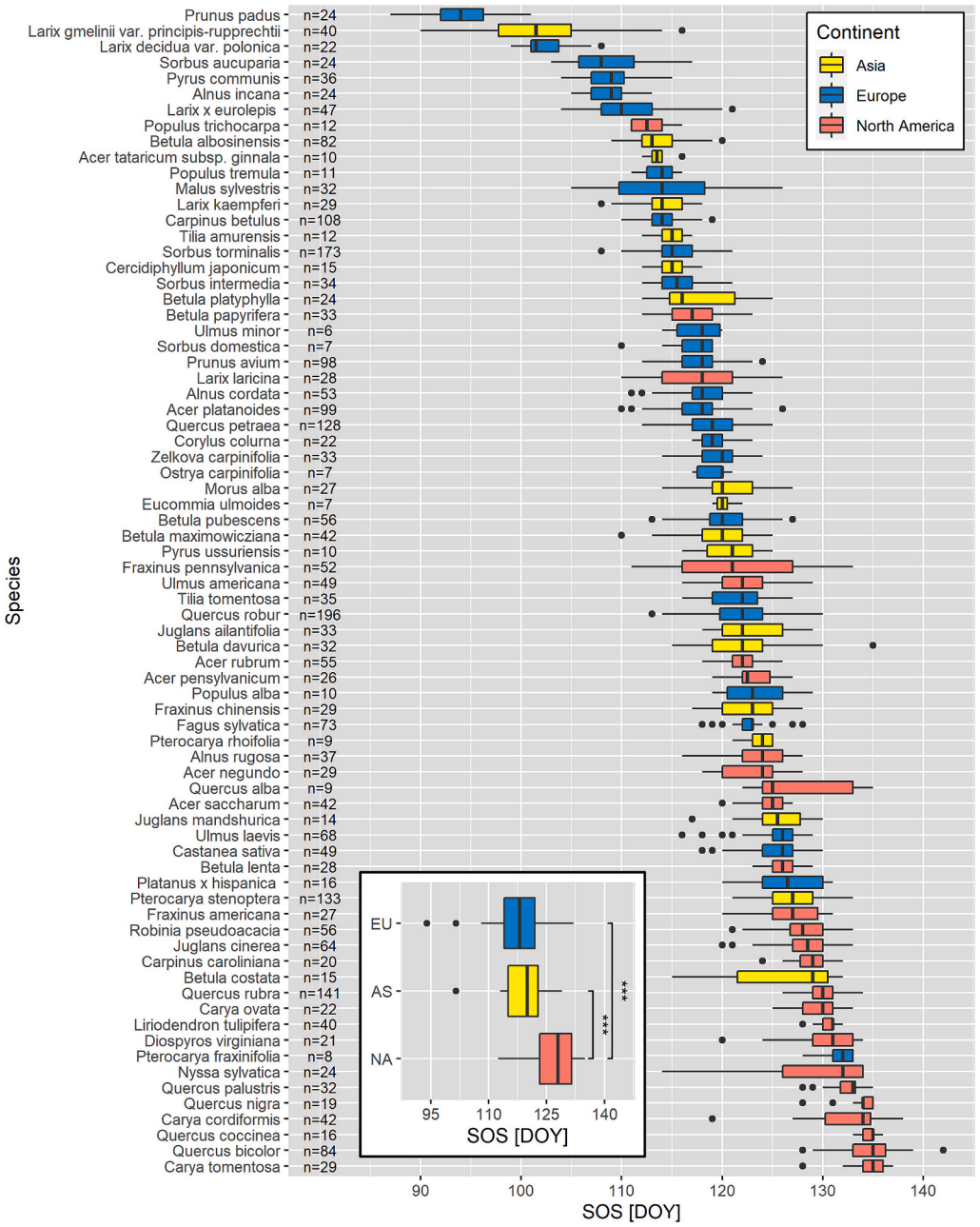

Fig. 4. Drone-derived SOS for the 74 tree species observed in the study area, ordered by median. The respective boxplots are composed of the SOS of the individuals and the tree species are colored according to the continent of origin (yellow: Asia; blue: Europe; red: North America). The number (n) of observed individuals of the respective tree species is indicated on the left-hand side. Small figure: SOS of the tree species of the respective continent of origin, which is composed of the medians of the large figure. The asterisks mark the significance of a two-sided Wilcoxon test between the respective continents (* = *p*-value <0.05; ** = p-value <0.01; *** = p-value <0.001, Bonferroni corrected).

interquartile range (IQR) of 11 days as well as *Betula costata* and *Quercus alba* with an IQR of 9 days each as the three most variable species). Notably the North American species leaved out significantly later compared to species of the other two continents (10-day difference to Europe in the median and 8 days to Asia; Asia/North America: W = 82.5, $p < 0.001$; Europe/North America: W = 112, $p < 0.001$).

Autumn phenology (EOS) for the observed species extended from late August to mid-November. The median of the first (*Fraxinus pennsylvanica*, 18th of September) and the last senescing species (*Ostrya carpinifolia*, 7th of November) had a difference of 50 days (Fig. 5). As in spring, there were also considerable differences within the species (IQR of 19 days for *Larix kaempferi* and 18.5 and 16.5 days for *Populus alba* and *Larix x eurolepis*, respectively, as the three most variable species). When comparing the continental areas of origin, no significant phenological differences were found between the different continents.

The length of the growing season (LOS) calculated from SOS and EOS ranged from 108 to 213 days (Fig. 6). The difference between the median of the species with the shortest (*Fraxinus pennsylvanica*, 137 days) and the longest vegetation period (*Larix decidua var. polonica*, 196 days) was 59 days. As in spring, it should also be noted that a small proportion (approx. 14 %) of the species observed had a remarkably longer vegetation period than most of the other species (~>180 days LOS in Fig. 6). Here, too, there was considerable intraspecific variability (IQR of 20 days for *Larix kaempferi* and 19.5 and 17.75 for *Fraxinus pennsylvanica* and *Malus sylvestris*, respectively, as the three most variable species). From a continental origin perspective, European species had a

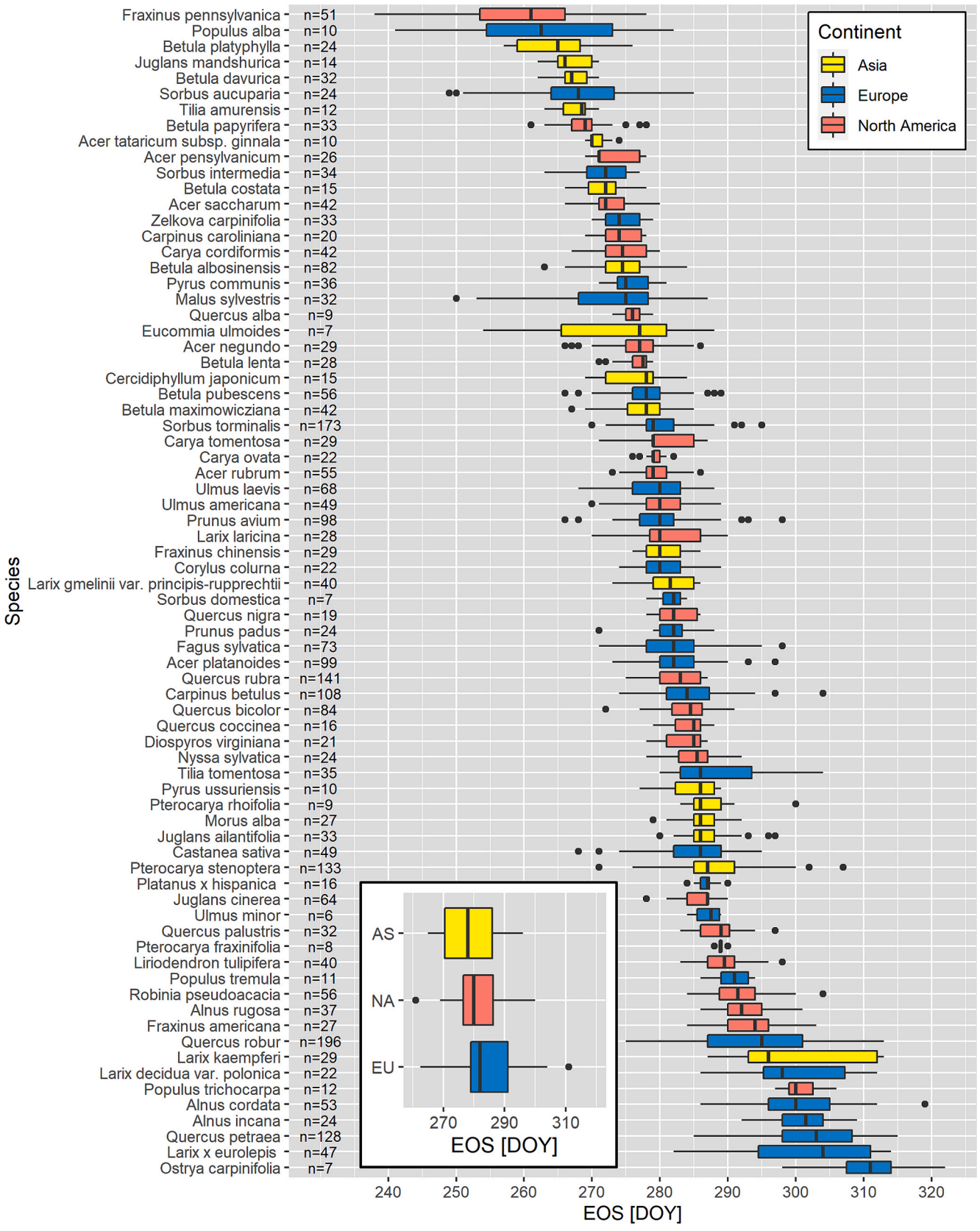

Fig. 5. Drone-derived EOS for the 74 tree species observed in the study area, ordered by median. The respective boxplots are composed of the EOS of the individuals and the tree species are colored according to the continent of origin (yellow: Asia; blue: Europe; red: North America). The number (n) of observed individuals of the respective tree species is indicated on the left-hand side. Small figure: EOS of the tree species of the respective continent of origin, which is composed of the medians of the large figure. The asterisks mark the significance of a two-sided Wilcoxon test between the respective continents (* = p-value <0.05; ** = p-value <0.01; *** = p-value <0.001, Bonferroni corrected).

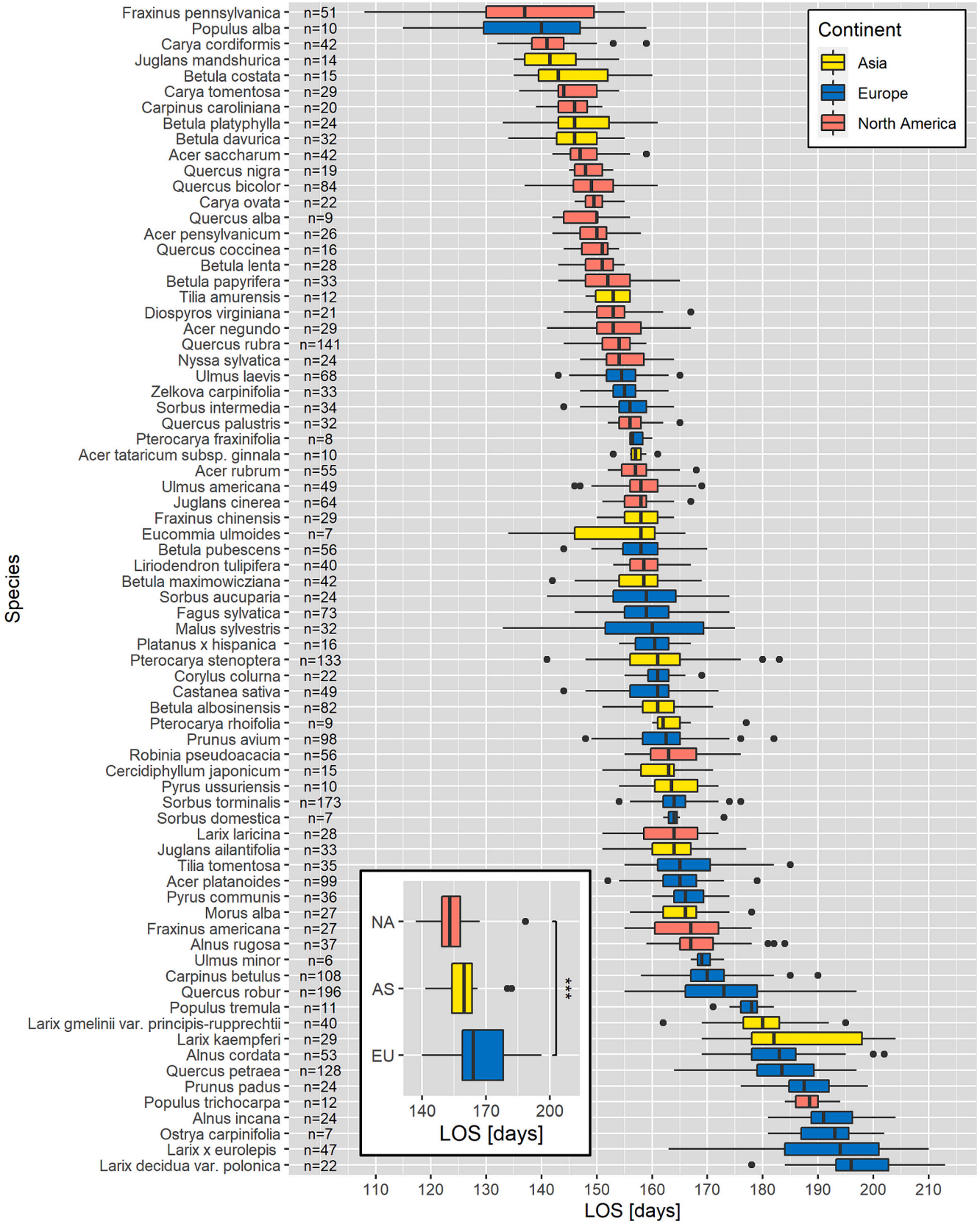

Fig. 6. Drone-derived LOS for the 74 tree species observed in the study area. Large figure: LOS of the respective tree species, ordered by median. The respective boxplots are composed of the LOS of the individuals and the tree species are colored according to the continent of origin (yellow: Asia; blue: Europe; red: North America). The number (n) of observed individuals of the respective tree species is indicated on the left-hand side. Small figure: LOS of the tree species of the respective continent of origin, which is composed of the medians of the large figure. The asterisks mark the significance of a two-sided Wilcoxon test between the respective continents (* = p-value <0.05; ** = p-value <0.01; *** = p-value <0.001, Bonferroni corrected).

significantly longer vegetation period than North American species (11-day difference in the median; $W = 653.5$, $p < 0.001$).

3.3. Relationship between phenology, functional traits, and climate distances

In the BRT analysis of the SOS and the functional traits as well as climate distance (cv correlation = 0.63), the three most important explanatory variables were the seed dry mass (relative influence: 20.2 %), the continent of origin (20.1 %) and the leaf thickness (12.8 %; Fig. 7a). If the tree species came from North America, a significant delay in SOS was observed, while the continents of Europe and Asia showed only minor differences (Fig. S7). A positive relationship between SOS and the traits mentioned was found for seed dry mass, with tree species with lighter seeds (<500 mg) leafing out earlier. In contrast, there was a negative relationship for leaf thickness, where later SOS was associated with tree species with a lower leaf thickness (<0.2 mm).

In the BRTs for EOS (cv correlation = 0.20), the number of chromosomes (15.7 %), the stem conduit diameter (15.7 %), and the SRL (12.6 %; Fig. 7b) were the three most important explanatory variables. A positive relationship between EOS and traits was found for stem conduit diameter, whereby an earlier EOS was more likely for tree species that had a smaller stem conduit diameter (<100 μm; Fig. S8). In contrast, the number of chromosomes and SRL had a negative relationship with EOS: tree species with fewer chromosomes (<20) and a lower SRL (<2000 cm g^{-1}) were more likely to be associated with a later EOS.

Finally, the BRT analysis for the LOS (cv correlation = 0.37) showed a combination of the results of SOS and EOS (Fig. 7c). The most important explanatory variables were the continent of origin (17.3 %), SRL (16.6 %) and seed dry mass (13.9 %). If the tree species came from

Fig. 7. Relative importance (%) of the functional traits and the climate distance for the individual phenological metrics (a: SOS; b: EOS; c: LOS) from the BRT analysis. Positive correlations between the respective traits and the phenological metrics are marked in green and negative correlations in red; the continent is marked in gray due to its three categorical characteristics. The corresponding partial dependency plots can be found in Figs. S7–9. The respective cv correlation was 0.63 (SOS), 0.20 (EOS) and 0.37 (LOS).

Europe, a significant longer LOS was observed, while the continents of Asia and North America showed only minor differences (Fig. S9). The other variables were negatively related to EOS, with tree species with lighter seeds (<50 mg) and a lower SRL (<2500 cm g^{-1}) being associated with a longer LOS.

4. Discussion

When assessing multiple phenological metrics using drone images across 74 deciduous tree species, both the drone-derived spring and, notably autumn phenology demonstrated a high degree of agreement with in-situ observations. A high inter- and intraspecific variability was found in the SOS, EOS, and LOS and a considerable part of the interspecific variability of up to 55 % can be related to functional traits, with the continent of origin, seed dry mass and number of chromosomes being among the most important ones.

4.1. Measuring deciduous tree phenology with a drone at a multi-species site: Possibilities and limitations

The drone spring and autumn crown phenology for a variety of deciduous tree species derived from a single uniform method (non-corrected NDVI values, double logistic function, "local" threshold) matched in-situ observations mostly well. This confirms previous studies (e.g., Klosterman and Richardson, 2017; Berra et al., 2019) reporting that reliable and robust recording of plant phenology at the individual level is possible by drone monitoring. Compared to similar study approaches (Budianti et al., 2021; Budianti et al., 2022; Fawcett et al., 2021; Wu et al., 2021), equal or even better agreements between drone- and in-situ-based phenology could be shown here, especially as these former studies even used different species, derivation methodologies and measurement devices.

The fact that the drone-based spring phenology shows less agreement with in-situ observations than the autumn phenology can be explained by the understory-overstory interaction: In spring, the understory vegetation shows an earlier greening compared to the adult tree crowns (e.g., Donnelly et al., 2024; Richardson and O'Keefe, 2009; Vitasse, 2013) and is therefore included in the (mixed-pixel) NDVI images of early spring. This temporal mismatch in spring is a general problem in remote sensing at different scales (e.g., Filippa et al., 2018; Ryu et al., 2014; Budianti et al., 2021; Donnelly et al., 2022), primarily explaining that NDVI data inconsistently predict an earlier SOS date than the observed onset of leaf unfolding. In autumn, however, the understory vegetation only influences the images after the leaves of the trees have fallen and therefore does not distort the drone-derived onset of senescence.

Tree species exhibiting a later SOS according to drone data compared to in-situ observations also underscore the methodological uncertainty inherent in phenological assessments. While drone-derived phenology addresses each individual tree, field observations rely on assumptions of representativeness for the plot, given that the entire area cannot be observed from the ground. In addition, ground truth data encompass specific phenological stages (such as budburst, leaf-out, and first leaf unfolded), whereas drone data only assesses a calculated index based on the greenness of the vegetation. This obviously leads to a larger discrepancy in spring compared to autumn phenology, as leaf discoloration is much easier monitored visually and on a larger scale. To increase the quality of drone-based phenological onset dates, a comparison with canopy or hemispherical camera images (as applied by Fawcett et al. (2021) or Klosterman et al. (2018)) can add more precision. Nevertheless, the evaluation results obtained in this study promise robust statements about key phases in the phenology of different tree species and their inter- and intraspecific variability.

4.2. Explaining intra- and interspecific variability of deciduous tree phenology

The trees exhibited high interspecific (up to 50-day difference in medians) and intraspecific (up to a 19-day interquartile range) phenological variability under nearly identical environmental conditions in both spring and autumn. This resulted in differences in the length of the growing season of up to almost two months between individual trees.

A large phenological variability of individuals within a tree species was also observed in previous analyses (e.g., Marchand et al., 2020; Delpierre et al., 2017; Prislan et al., 2013). The reasons for this intraspecific variability are often the age and height of the trees observed (Augspurger and Bartlett, 2003; Marchand et al., 2020; Osada and Hiura, 2019), but also the microclimate (Delpierre et al., 2017; Osada and Hiura, 2019) and genetic diversity (Capdevielle-Vargas et al., 2015; Delpierre et al., 2017; Schmeddes et al., 2023). In our study area, all individuals of a tree species are planted in the same year and therefore differ only slightly in height, which is why the variability cannot be explained by the previous factors. Temporal patterns (as later leaf-out and earlier senescence mean less variability; Denéchère et al., 2021) are also not observable in both spring and autumn. In contrast, the large intraspecific variability is striking. In addition, as in comparable studies (e.g., Denéchère et al., 2021; Marchand et al., 2020; Capdevielle-Vargas et al., 2015), the intraspecific variability is lower in spring than in autumn events. This can be explained by the fact that the onset of senescence is more complex and therefore dependent on more factors than spring phenology (Gill et al., 2015; Lu and Keenan, 2022). Accordingly, the sensitivity to individual drivers can have accumulated effects on different individuals and thus result in greater autumnal phenological plasticity.

Comparing the phenological onset dates between the species, the interspecific phenological variability in spring was in line with previous studies (e.g., Cole and Sheldon, 2017; Panchen et al., 2014; Richardson and O'Keefe, 2009; Wesołowski and Rowiński, 2006). In contrast, the variability of autumn phenology was comparatively high (e.g., compared to Budianti et al., 2022; Budianti et al., 2021; Wu et al., 2021; Archetti et al., 2013; Richardson and O'Keefe, 2009), which can be explained by the high number and diversity of the species considered. Even though a comparison with other studies is only possible to a limited extent due to different meteorological and environmental conditions, parallels can be recognized in the chronological order of the phenological onset dates of the tree species: While species such as *Alnus incana* (Donnelly et al., 2017) or the genera *Prunus*, *Populus* (Richardson and O'Keefe, 2009) or *Corylus* (Wesołowski and Rowiński, 2006) tend to leaf out early, greening of *Nyssa sylvatica* or the genera *Quercus* (Richardson and O'Keefe, 2009) and *Fraxinus* (Cole and Sheldon, 2017) are more likely to be observed later in the spring. In autumn, on the other hand, early leaf discoloration seems to be common, especially in *Acer rubrum* (Archetti et al., 2013; Richardson and O'Keefe, 2009), while the genera *Populus* and *Quercus* mainly senesce later in the year (Archetti et al., 2013; Richardson and O'Keefe, 2009; Wu et al., 2021).

Both in spring and in autumn, the variation in phenological timing between the tree species can be interpreted as different growth strategies: While early leafing-out plant genera such as *Larix* or various species of the Rosaceae family (*Prunus padus*, *Pyrus communis*, *Sorbus aucuparia*, *Malus sylvestris*) or late senescing genera such as *Larix* or *Quercus* pursue maximization of carbon sequestration and use of seasonally limited resources (i.e., light) over a prolonged growth period ("phenological escape"; e.g., Lee and Ibáñez, 2021; Richardson and O'Keefe, 2009), genera such as *Quercus* or *Carya* presumably try to minimize the risk of late frost by late leaf emergence in spring (Bennie et al., 2010; Vitasse et al., 2014).

These strategies seem to have some inherent logic, but the phenological behavior of a specific single species is difficult to derive from these general statements. One possibility is to link the growth strategies to continents of origin and to the respective functional traits of the tree

species. Our study shows that North American tree species and species with higher seed dry mass and lower leaf thickness are associated with later leaf-out. Interestingly, other studies have also linked the time of leaf emergence or phenological sensitivity to continental differences (Lee et al., 2022; Zohner and Renner, 2017), whereby a later leaf-out in North American species is primarily explained by higher variability of North American spring temperatures and the associated risk avoidance strategy with regard to late frost events (Zohner et al., 2017). In contrast to Zohner and Renner (2017) earlier leaf discoloration of North American species is hardly observed in our study. Frost avoidance could also be the driver for other traits: tree species with heavier seeds may invest a lot of energy in reproduction and are therefore more likely to lower risks associated with energy loss due to late frost. Furthermore, tree species with thinner leaves are more susceptible to low temperatures and the resulting frost damage (Bucher et al., 2019; Bucher and Rosbakh, 2021) and therefore may exhibit a later leaf-out date, similar to Horbach et al. (2023).

A significantly distinct picture emerges when considering traits related to autumn phenology: tree species with a lower chromosome number and SRL as well as a larger stem conduit diameter tend to enter senescence later. A potential influence of chromosome numbers represents a totally novel aspect in plant phenology, with only a few papers offering insights into potential explanatory connections. For example, it is known that species with monoploid large genomes are more likely to invest in inflorescence preformation and thus flower and senesce earlier (Schnablová et al., 2021). In principle, different chromosome numbers in angiosperm tree genera hint at phylogenetic differences (Carta et al., 2018). Interestingly, for Italian vascular plant species, chromosome numbers were poorly related to climatic conditions, but to environmental categorical variables suggesting an evolutionary role. Carta et al. (2018) reported that lower chromosome numbers were associated with open, disturbed, drought-prone, i.e. instable habitats, while species in stable environments (favoring higher recombination rates) and with longer life cycles had generally higher chromosome numbers. Translating our findings into Carta's scheme would indicate that species from stable environments should have EOS earlier, whereas pioneers or species from disturbed habitats may profit from later EOS. With regard to the stem conduit diameter, due to the positive correlation with both spring and autumn phenology, it can be assumed that the species that unfolded their leaves later due to the strategy of frost avoidance with a larger conduit diameter (Lechowicz, 1984; Panchen et al., 2014) now make up for the initially lower carbon sequestration compared to other species through later senescence. Regarding SRL, our findings might be linked to nutrient and water acquisition as good water-use efficiency was linked to later dates of senescence (Bucher and Römermann, 2021).

Another aspect that should also be mentioned in this context is the drought summer of 2022 (Toreti et al., 2022). Regarding the general influence of drought on autumn phenology, the current study situation is contradictory (Gill et al., 2015; Lu and Keenan, 2022; Zani et al., 2020), with tree species' phenology reacting individually to drought stress (Bigler and Vitasse, 2021; Grossiord et al., 2022). Both visually in the field and in the NDVI data, no drought stress could be detected within the plots of the study area in the summer of 2022, most likely due to optimal soils with high water storage capacities, which meant that no analyses could be carried out in this context. Nevertheless, this circumstance should be included in the final assessment when considering autumn phenological variability.

The length of the growing season, which results from SOS and EOS, is a clear combination of the SOS/EOS-trait relationships. European species start leaf emergence earliest and change color later than North American and Asian species, resulting in a significantly longer growing season. SOS responses to chilling and forcing are suggested to be a result of an adaptation to the predictability of the winter-spring transition and late spring frosts (e.g. Zohner et al., 2017 or Walde et al., 2022), which should result, given sufficient chilling, in a stronger coupling to forcing of Northeastern Asia to Europe (Walde et al., 2022) and or Europe to North America (Zohner et al., 2017). LOS variations are associated with further traits, such as SRL, where a higher value is associated with earlier senescence and thus a shorter LOS. Finally, a high seed dry mass tends to result in later leaf emergence, which also results in a shorter LOS.

4.3. Limitations and uncertainties

Due to the large number of trait data sets and the complex methodology to derive single tree crown phenological onset dates, there are also several uncertainties and limitations in our study. Regarding the drone data it should be noted that there are different illumination conditions depending on the season and weather, which can influence the calculation of the NDVI values (Fawcett et al., 2021). In addition, the orthorectification also induces inaccuracies of up to 30 cm, which can primarily distort the edge pixels of the respective crowns. The in-situ observations were only observed plot-wise. As shown in the study though, there are clear intraspecific phenological differences, which cannot be described in a plot-by-plot summary. Not all individuals were clearly visible, especially in larger plots, which made the assessment even more difficult. In addition, only a subset of the species analyzed with the drone could be observed on the ground and the temporal frequency of the drone and in-situ data do not match. Regarding the functional traits used in the study, most of the traits were not measured on-site, but were only retrieved from database values, of which some were based on a gap-filling algorithm. Different values would certainly be measured on site, although the magnitude of the values should be realistic depending on the species (e.g., Kazakou et al., 2014; Cordlandwehr et al., 2013; Violle et al., 2015).

Regarding the methodology, it is particularly noteworthy that the polygons of the respective tree crowns are created automatically and therefore only represent the real crown shape to a limited extent, even if unrealistic crowns were removed in the selection process. With >3000 individuals, we cannot rule out with 100 % certainty that another species has spread naturally somewhere in the plots and - due to very similar phenology - this individual has not been noticed. When extracting the phenology from the drone images, curve fitting represents a simplification of the phenological curve, but is also a well-accepted (Zeng et al., 2020) method to reduce the influence of false outliers (snow cover, drought influence). In addition, setting a general NDVI threshold for over 3000 individuals and 74 species is a clear simplification of the phenological conditions and a comparative calculation of phenological metrics with other vegetation indices would represent an interesting perspective for further research. Regarding the BRT, it should be noted that models based on 74 data points (species) do not promise the highest robustness but are appropriate in this context. Finally, the fact that only the phenology of a single year was observed in this study should also be taken into account when interpreting the results. While the chronological order of the phenological onset times of the observed tree species should also remain roughly the same in other years (e.g., Cole and Sheldon, 2017; Archetti et al., 2013; Wesołowski and Rowiński, 2006), differences to other years can also arise depending on weather conditions and the climatic sensitivity of the species, and thus may slightly alter the results obtained.

5. Conclusion

Analyzing the phenology of 74 deciduous tree species and 3099 individuals using drone images, our study generates important new insights from both technical and ecophysiological perspectives. We showed that the derivation of SOS, EOS, and LOS via drone images for a large number of tree species using just one methodology achieves robust results and is a promising approach for monitoring phenology on the tree-individual level. Significant phenological differences were found both within and between tree species, which led to differences in the length of the growing season of up to two months under nearly identical

environmental conditions. The interspecific phenological variation could be explained by functional traits, with the continent of origin, seed dry mass and leaf thickness in spring explaining the variability with the strategy of frost avoidance. In autumn, the number of chromosomes, the SRL and the stem conduit diameter played a dominant role. The results encourage new research approaches in the field of plant phenology and form an important basis for understanding different growth strategies of dominant deciduous tree species in the Northern Hemisphere. Finally, the methodological support with camera data and traits measured on-site offer further potential to generate in-depth phenological insights within this research field in the future.

CRediT authorship contribution statement

Simon Kloos: Writing – review & editing, Writing – original draft, Visualization, Validation, Software, Methodology, Investigation, Formal analysis, Data curation, Conceptualization. **Marvin Lüpke:** Writing – review & editing, Writing – original draft, Validation, Software, Resources, Methodology, Investigation, Data curation. **Nicole Estrella:** Writing – review & editing, Supervision. **Wael Ghada:** Writing – review & editing, Investigation, Data curation. **Jens Kattge:** Writing – review & editing, Investigation, Data curation. **Solveig Franziska Bucher:** Writing – review & editing, Methodology, Formal analysis. **Allan Buras:** Writing – review & editing, Writing – original draft, Investigation, Data curation. **Annette Menzel:** Writing – review & editing, Supervision, Project administration, Methodology, Investigation, Funding acquisition, Conceptualization.

Declaration of competing interest

The authors declare that they have no known competing financial interests or personal relationships that could have appeared to influence the work reported in this paper.

Data availability

The phenological and trait-related data that support the findings of this study and the R code regarding the extraction of the phenological metrics are openly available in *figshare* (DOI: https://doi.org/10.6084/m9.figshare.24926256). Further data sets from this study are available on request.

Acknowledgments

The authors would like to thank the Bavarian State Forests (BaySF) and the Bavarian State Institute of Forestry for the permission to conduct research in Weltwald Freising and for the provision and use of study area data. Furthermore, we would like to thank all supporters of the drone monitoring, here notably Niklas Kessel for operating many drone flights during spring and testing different tree detection and canopy delineation algorithms. For the phenological ground observations, we especially thank Yahya Ghalayini, Teresa Mühlbauer, Katharina Brückl, and Louise Harms.

Funding information

This work was supported by the Bavarian State Ministry of Science and the Arts (F.7-F5121.14.2.3/14/6) in the context of the Bavarian Climate Research Network (bayklif) within the project BAYSICS (Bavarian Citizen Science Portal for Climate Research and Science Communication). Additionally, funding from the Bavarian State Ministry of Food, Agriculture and Forestry (StMELF) (klifW013: 7831-1/1014, klifW012: 7831-1/1078, and project M029) was received.

Appendix A. Supplementary data

Supplementary data to this article can be found online at https://doi.org/10.1016/j.scitotenv.2024.175753.

References

Archetti, M., Richardson, A.D., O'Keefe, J., Delpierre, N., 2013. Predicting climate change impacts on the amount and duration of autumn colors in a New England forest. PLoS One 8 (3), e57373. https://doi.org/10.1371/journal.pone.0057373.

Augspurger, C.K., Bartlett, E.A., 2003. Differences in leaf phenology between juvenile and adult trees in a temperate deciduous forest. Tree Physiol. 23 (8), 517–525. https://doi.org/10.1093/treephys/23.8.517.

Bavarian State Forestry, 2022. (C) Geodata. https://services1.arcgis.com/dzpA3ZtAF0zx03DV/arcgis/rest/services/Weltwald_Update_05_2022/FeatureServer (accessed 10 January 2024).

Bennie, J., Kubin, E., Wiltshire, A., Huntley, B., Baxter, R., 2010. Predicting spatial and temporal patterns of bud-burst and spring frost risk in north-west Europe: the implications of local adaptation to climate. Glob. Chang. Biol. 16 (5), 1503–1514. https://doi.org/10.1111/j.1365-2486.2009.02095.x.

Berra, E.F., Gaulton, R., 2021. Remote sensing of temperate and boreal forest phenology: a review of progress, challenges and opportunities in the intercomparison of in-situ and satellite phenological metrics. For. Ecol. Manag. 480, 118663. https://www.sciencedirect.com/science/article/pii/S0378112720314328.

Berra, E.F., Gaulton, R., Barr, S., 2019. Assessing spring phenology of a temperate woodland: a multiscale comparison of ground, unmanned aerial vehicle and Landsat satellite observations. Remote Sens. Environ. 223, 229–242. https://doi.org/10.1016/j.rse.2019.01.010.

Bigler, C., Vitasse, Y., 2021. Premature leaf discoloration of European deciduous trees is caused by drought and heat in late spring and cold spells in early fall. Agric. For. Meteorol. 307, 108492 https://doi.org/10.1016/j.agrformet.2021.108492.

Bolmgren, K., Cowan, P.D., 2008. Time – size tradeoffs: a phylogenetic comparative study of flowering time, plant height and seed mass in a north-temperate flora. Oikos 117 (3), 424–429. https://doi.org/10.1111/j.2007.0030-1299.16142.x.

Bucher, S.F., Römermann, C., 2021. The timing of leaf senescence relates to flowering phenology and functional traits in 17 herbaceous species along elevational gradients. J. Ecol. 109 (3), 1537–1548. https://doi.org/10.1111/1365-2745.13577.

Bucher, S.F., Rosbakh, S., 2021. Foliar summer frost resistance measured via electrolyte leakage approach as related to plant distribution, community composition and plant traits. Funct. Ecol. 35 (3), 590–600. https://doi.org/10.1111/1365-2435.13740.

Bucher, S.F., König, P., Menzel, A., Migliavacca, M., Ewald, J., Römermann, C., 2018. Traits and climate are associated with first flowering day in herbaceous species along elevational gradients. Ecol. Evol. 8 (2), 1147–1158. https://doi.org/10.1002/ece3.3720.

Bucher, S.F., Feiler, R., Buchner, O., Neuner, G., Rosbakh, S., Leiterer, M., et al., 2019. Temporal and spatial trade-offs between resistance and performance traits in herbaceous plant species. Environ. Exp. Bot. 157, 187–196. https://doi.org/10.1016/j.envexpbot.2018.10.015.

Budianti, N., Mizunaga, H., Iio, A., 2021. Crown structure explains the discrepancy in leaf phenology metrics derived from ground- and UAV-based observations in a Japanese cool temperate deciduous forest. Forests 12 (4), 425. https://doi.org/10.3390/f12040425.

Budianti, N., Naramoto, M., Iio, A., 2022. Drone-sensed and sap flux-derived leaf phenology in a cool temperate deciduous forest: a tree-level comparison of 17 species. Remote Sens. 14 (10), 2505. https://doi.org/10.3390/rs14102505.

Buras, A., Menzel, A., 2019. Projecting tree species composition changes of European forests for 2061-2090 under RCP 4.5 and RCP 8.5 scenarios. Front. Plant Sci. 9, 1986 https://doi.org/10.3389/fpls.2018.01986.

Capdevielle-Vargas, R., Estrella, N., Menzel, A., 2015. Multiple-year assessment of phenological plasticity within a beech (Fagus sylvatica L.) stand in southern Germany. Agric. For. Meteorol. 211–212, 13–22. https://doi.org/10.1016/j.agrformet.2015.03.019.

Carta, A., Bedini, G., Peruzzi, L., 2018. Unscrambling phylogenetic effects and ecological determinants of chromosome number in major angiosperm clades. Sci. Rep. 8 (1), 14258 https://doi.org/10.1038/s41598-018-32515-x.

Caudullo, G., Welk, E., San-Miguel-Ayanz, J., 2017. Chorological maps for the main European woody species. Data Brief 12, 662–666. https://doi.org/10.1016/j.dib.2017.05.007.

Cleland, E.E., Chuine, I., Menzel, A., Mooney, H.A., Schwartz, M.D., 2007. Shifting plant phenology in response to global change. Trends Ecol. Evol. 22 (7), 357–365. https://www.cell.com/trends/ecology-evolution/fulltext/s0169-5347(07)00130-9.

Cole, E.F., Sheldon, B.C., 2017. The shifting phenological landscape: within- and between-species variation in leaf emergence in a mixed-deciduous woodland. Ecol. Evol. 7 (4), 1135–1147. https://doi.org/10.1002/ece3.2718.

Cordlandwehr, V., Meredith, R.L., Ozinga, W.A., Bekker, R.M., van Groenendael, J.M., Bakker, J.P., 2013. Do plant traits retrieved from a database accurately predict on-site measurements? J. Ecol. 101 (3), 662–670. https://doi.org/10.1111/1365-2745.12091.

Craine, J.M., Wolkovich, E.M., Gene Towne, E., Kembel, S.W., 2012. Flowering phenology as a functional trait in a tallgrass prairie. New Phytol. 193 (3), 673–682. https://doi.org/10.1111/j.1469-8137.2011.03953.x.

Dalponte, M., Coomes, D.A., 2016. Tree-centric mapping of forest carbon density from airborne laser scanning and hyperspectral data. Methods Ecol. Evol. 7 (10), 1236–1245. https://doi.org/10.1111/2041-210X.12575.

Dandois, J.P., Ellis, E.C., 2013. High spatial resolution three-dimensional mapping of vegetation spectral dynamics using computer vision. Remote Sens. Environ. 136, 259–276. https://doi.org/10.1016/j.rse.2013.04.005.
Delpierre, N., Guillemot, J., Dufrêne, E., Cecchini, S., Nicolas, M., 2017. Tree phenological ranks repeat from year to year and correlate with growth in temperate deciduous forests. Agric. For. Meteorol. 234–235, 1–10. https://doi.org/10.1016/j.agrformet.2016.12.008.
Denéchère, R., Delpierre, N., Apostol, E.N., Berveiller, D., Bonne, F., Cole, E., et al., 2021. The within-population variability of leaf spring and autumn phenology is influenced by temperature in temperate deciduous trees. Int. J. Biometeorol. 65 (3), 369–379. https://doi.org/10.1007/s00484-019-01762-6.
Diez, J.M., Ibáñez, I., Miller-Rushing, A.J., Mazer, S.J., Crimmins, T.M., Crimmins, M.A., et al., 2012. Forecasting phenology: from species variability to community patterns. Ecol. Lett. 15 (6), 545–553. https://doi.org/10.1111/j.1461-0248.2012.01765.x.
Donnelly, A., Yu, R., Caffarra, A., Hanes, J., Liang, L., Desai, A.R., et al., 2017. Interspecific and interannual variation in the duration of spring phenophases in a northern mixed forest. Agric. For. Meteorol. 243, 55–67. https://doi.org/10.1016/j.agrformet.2017.05.007.
Donnelly, A., Yu, R., Jones, K., Belitz, M., Li, B., Duffy, K., Zhang, X., Wang, J., Seyednasrollah, B., Gerst, K.L., Li, D., Kaddoura, Y., Zhu, K., Morisette, J., Ramey, C., Smith, K., 2022. Exploring discrepancies between in situ phenology and remotely derived phenometrics at NEON sites. Ecosphere 13 (1), e3912. https://doi.org/10.1002/ecs2.3912.
Donnelly, A., Yu, R., Rehberg, C., Schwartz, M.D., 2024. Characterizing spring phenology in a temperate deciduous urban woodland fragment: trees and shrubs. Int. J. Biometeorol. 68 (5), 871–882. https://doi.org/10.1007/s00484-024-02632-6.
Dorji, T., Totland, O., Moe, S.R., Hopping, K.A., Pan, J., Klein, J.A., 2013. Plant functional traits mediate reproductive phenology and success in response to experimental warming and snow addition in Tibet. Glob. Chang. Biol. 19 (2), 459–472. https://doi.org/10.1111/gcb.12059.
Du, G., Qi, W., 2010. Trade-offs between flowering time, plant height, and seed size within and across 11 communities of a QingHai-Tibetan flora. Plant Ecol. 209 (2), 321–333. https://doi.org/10.1007/s11258-010-9763-4.
DWD, 2024. Historische tägliche Stationsbeobachtungen (Temperatur, Druck, Niederschlag, Sonnenscheindauer, etc.) für Deutschland, Version v23.3: München-Flughafen. https://opendata.dwd.de/climate_environment/CDC/observations_germany/climate/daily/kl/historical/ (accessed 13 March 2024).
Elith, J., Leathwick, J.R., Hastie, T., 2008. A working guide to boosted regression trees. J. Anim. Ecol. 77 (4), 802–813. https://doi.org/10.1111/j.1365-2656.2008.01390.x.
Ettinger, A.K., Chamberlain, C.J., Morales-Castilla, I., Buonaiuto, D.M., Flynn, D.F.B., Savas, T., et al., 2020. Winter temperatures predominate in spring phenological responses to warming. Nat. Clim. Chang. 10 (12), 1137–1142. https://doi.org/10.1038/s41558-020-00917-3.
Fawcett, D., Bennie, J., Anderson, K., 2021. Monitoring spring phenology of individual tree crowns using drone-acquired NDVI data. Remote Sens. Ecol. Conserv. 7 (2), 227–244. https://doi.org/10.1002/rse2.184.
Filippa, G., Cremonese, E., Migliavacca, M., Galvagno, M., Sonnentag, O., Humphreys, E., et al., 2018. NDVI derived from near-infrared-enabled digital cameras: applicability across different plant functional types. Agric. For. Meteorol. 249, 275–285. https://doi.org/10.1016/j.agrformet.2017.11.003.
Fischer, A., 1994. A model for the seasonal variations of vegetation indices in coarse resolution data and its inversion to extract crop parameters. Remote Sens. Environ. 48 (2), 220–230. https://www.sciencedirect.com/science/article/pii/0034425794901430.
Flynn, D.F.B., Wolkovich, E.M., 2018. Temperature and photoperiod drive spring phenology across all species in a temperate forest community. New Phytol. 219 (4), 1353–1362. https://doi.org/10.1111/nph.15232.
Gaertner, B.A., Zegre, N., Warner, T., Fernandez, R., He, Y., Merriam, E.R., 2019. Climate, forest growing season, and evapotranspiration changes in the central Appalachian Mountains, USA. Sci. Total Environ. 650 (Pt 1), 1371–1381. https://doi.org/10.1016/j.scitotenv.2018.09.129.
Garonna, I., Jong, R. de, Schaepman, M.E., 2016. Variability and evolution of global land surface phenology over the past three decades (1982-2012). Glob. Chang. Biol. 22 (4), 1456–1468. https://doi.org/10.1111/gcb.13168.
Gill, A.L., Gallinat, A.S., Sanders-DeMott, R., Rigden, A.J., Short Gianotti, D.J., Mantooth, J.A., et al., 2015. Changes in autumn senescence in northern hemisphere deciduous trees: a meta-analysis of autumn phenology studies. Ann. Bot. 116 (6), 875–888. https://doi.org/10.1093/aob/mcv055.
Global Biodiversity Information Facility, 2021. Free and open access to biodiversity data. https://www.gbif.org/ (accessed 08 November 2023).
Gressler, E., Jochner, S., Capdevielle-Vargas, R.M., Morellato, L.P.C., Menzel, A., 2015. Vertical variation in autumn leaf phenology of Fagus sylvatica L. in southern Germany. Agric. For. Meteorol. 201, 176–186. https://doi.org/10.1016/j.agrformet.2014.10.013.
Grossiord, C., Bachofen, C., Gisler, J., Mas, E., Vitasse, Y., Didion-Gency, M., 2022. Warming may extend tree growing seasons and compensate for reduced carbon uptake during dry periods. J. Ecol. 110 (7), 1575–1589. https://doi.org/10.1111/1365-2745.13892.
Harris, I., Osborn, T.J., Jones, P., Lister, D., 2020. Version 4 of the CRU TS monthly high-resolution gridded multivariate climate dataset. Sci. Data 7 (1), 109. https://doi.org/10.1038/s41597-020-0453-3.
Hijmans, R.J., Phillips, S., Leathwick, J., Elith, J., 2023. Package 'dismo'. https://cran.r-project.org/web/packages/dismo/index.html (accessed 02 November 2023).
Horbach, S., Rauschkolb, R., Römermann, C., 2023. Flowering and leaf phenology are more variable and stronger associated to functional traits in herbaceous compared to tree species. Flora 300, 152218. https://doi.org/10.1016/j.flora.2023.152218.
Kattge, J., Bönisch, G., Díaz, S., Lavorel, S., Prentice, I.C., Leadley, P., et al., 2020. TRY plant trait database - enhanced coverage and open access. Glob. Chang. Biol. 26 (1), 119–188. https://doi.org/10.1111/gcb.14904.
Kazakou, E., Violle, C., Roumet, C., Navas, M.-L., Vile, D., Kattge, J., et al., 2014. Are trait-based species rankings consistent across data sets and spatial scales? J. Veg. Sci. 25 (1), 235–247. https://doi.org/10.1111/jvs.12066.
Keenan, T.F., Gray, J., Friedl, M.A., Toomey, M., Bohrer, G., Hollinger, D.Y., et al., 2014. Net carbon uptake has increased through warming-induced changes in temperate forest phenology. Nat. Clim. Chang. 4 (7), 598–604. https://doi.org/10.1038/nclimate2253.
Kim, J.H., Hwang, T., Yang, Y., Schaaf, C.L., Boose, E., Munger, J.W., 2018. Warming-induced earlier greenup leads to reduced stream discharge in a temperate mixed forest catchment. JGR Biogeosci. 123 (6), 1960–1975. https://doi.org/10.1029/2018JG004438.
Kleinsmann, J., Verbesselt, J., Kooistra, L., 2023. Monitoring individual tree phenology in a multi-species forest using high resolution UAV images. Remote Sens. 15 (14), 3599. https://doi.org/10.3390/rs15143599.
Kloos, S., Klosterhalfen, A., Knohl, A., Menzel, A., 2024. Decoding autumn phenology: unraveling the link between observation methods and detected environmental cues. Glob. Chang. Biol. 30 (3) https://doi.org/10.1111/gcb.17231.
Klosterman, S., Richardson, A.D., 2017. Observing spring and fall phenology in a deciduous forest with aerial drone imagery. Sensors 17 (12). https://doi.org/10.3390/s17122852.
Klosterman, S., Melaas, E., Wang, J.A., Martinez, A., Frederick, S., O'Keefe, J., et al., 2018. Fine-scale perspectives on landscape phenology from unmanned aerial vehicle (UAV) photography. Agric. For. Meteorol. 248, 397–407. https://doi.org/10.1016/j.agrformet.2017.10.015.
König, P., Tautenhahn, S., Cornelissen, J.H.C., Kattge, J., Bönisch, G., Römermann, C., 2018. Advances in flowering phenology across the Northern Hemisphere are explained by functional traits. Glob. Ecol. Biogeogr. 27 (3), 310–321. https://doi.org/10.1111/geb.12696.
Körner, C., Möhl, P., Hiltbrunner, E., 2023. Four ways to define the growing season. Ecol. Lett. 26 (8), 1277–1292. https://doi.org/10.1111/ele.14260.
Lange, M., Doktor, D., 2022. Package 'phenex'. https://cran.r-project.org/web/packages/phenex/index.html (accessed 31 October 2023).
Lauterbach, D., Römermann, C., Jeltsch, F., Ristow, M., 2013. Factors driving plant rarity in dry grasslands on different spatial scales: a functional trait approach. Biodivers. Conserv. 22 (10), 2337–2352. https://doi.org/10.1007/s10531-013-0455-y.
Lechowicz, M.J., 1984. Why do temperate deciduous trees leaf out at different times? Adaptation and ecology of forest communities. Am. Nat. 124 (6), 821–842. https://doi.org/10.1086/284319.
Lee, B.R., Ibáñez, I., 2021. Spring phenological escape is critical for the survival of temperate tree seedlings. Funct. Ecol. 35 (8), 1848–1861. https://doi.org/10.1111/1365-2435.13821.
Lee, B.R., Miller, T.K., Rosche, C., Yang, Y., Heberling, J.M., Kuebbing, S.E., et al., 2022. Wildflower phenological escape differs by continent and spring temperature. Nat. Commun. 13 (1), 7157. https://doi.org/10.1038/s41467-022-34936-9.
Liu ZhiGuo, Kai, Li, YongLi, Cai, Yan, Fang, 2011. Correlations between leafing phenology and traits: woody species of evergreen broad-leaved forests in subtropical China. Pol. J. Ecol. 59 (3), 463–473.
Liu, Y., Li, G., Wu, X., Niklas, K.J., Yang, Z., Sun, S., 2021. Linkage between species traits and plant phenology in an alpine meadow. Oecologia 195 (2), 409–419. https://doi.org/10.1007/s00442-020-04846-y.
Louault, F., Pillar, v.d., Aufrère, J., Garnier, E., Soussana, J.-F., 2005. Plant traits and functional types in response to reduced disturbance in a semi-natural grassland. J. Veg. Sci. 16 (2), 151–160. https://doi.org/10.1111/j.1654-1103.2005.tb02350.x.
Lu, X., Keenan, T.F., 2022. No evidence for a negative effect of growing season photosynthesis on leaf senescence timing. Glob. Chang. Biol. 28 (9), 3083–3093. https://doi.org/10.1111/gcb.16104.
Marchand, L.J., Dox, I., Gričar, J., Prislan, P., Leys, S., van den Bulcke, J., et al., 2020. Inter-individual variability in spring phenology of temperate deciduous trees depends on species, tree size and previous year autumn phenology. Agric. For. Meteorol. 290, 108031 https://doi.org/10.1016/j.agrformet.2020.108031.
Melaas, E.K., Sulla-Menashe, D., Friedl, M.A., 2018. Multidecadal changes and interannual variation in springtime phenology of North American temperate and boreal deciduous forests. Geophys. Res. Lett. 45 (6), 2679–2687. https://doi.org/10.1002/2017GL076933.
Menzel, A., Sparks, T.H., Estrella, N., Koch, E., Aasa, A., Ahas, R., et al., 2006. European phenological response to climate change matches the warming pattern. Glob. Chang. Biol. 12 (10), 1969–1976. https://doi.org/10.1111/j.1365-2486.2006.01193.x.
Menzel, A., Yuan, Y., Matiu, M., Sparks, T., Scheifinger, H., Gehrig, R., et al., 2020. Climate change fingerprints in recent European plant phenology. Glob. Chang. Biol. https://doi.org/10.1111/gcb.15000.
Osada, N., Hiura, T., 2019. Intraspecific differences in spring leaf phenology in relation to tree size in temperate deciduous trees. Tree Physiol. 39 (5), 782–791. https://doi.org/10.1093/treephys/tpz011.
Panchen, Z.A., Primack, R.B., Nordt, B., Ellwood, E.R., Stevens, A.-D., Renner, S.S., et al., 2014. Leaf out times of temperate woody plants are related to phylogeny, deciduousness, growth habit and wood anatomy. New Phytol. 203 (4), 1208–1219. https://doi.org/10.1111/nph.12892.
Piao, S., Friedlingstein, P., Ciais, P., Viovy, N., Demarty, J., 2007. Growing season extension and its impact on terrestrial carbon cycle in the Northern Hemisphere over

the past 2 decades. Glob. Biogeochem. Cycles 21 (3). https://doi.org/10.1029/2006GB002888.
Piao, S., Liu, Q., Chen, A., Janssens, I.A., Fu, Y., Dai, J., et al., 2019. Plant phenology and global climate change: current progresses and challenges. Glob. Chang. Biol. 25 (6), 1922–1940. https://doi.org/10.1111/gcb.14619.
Plowright, A., Roussel, J.-R., 2023. Package 'ForestTools'. https://cran.r-project.org/web/packages/ForestTools/index.html (accessed 07 November 2023).
Popescu, S.C., Wynne, R.H., 2004. Seeing the trees in the forest. Photogramm. Eng. Remote Sens. 70 (5), 589–604. https://doi.org/10.14358/PERS.70.5.589.
Prislan, P., Gričar, J., Luis, M. de, Smith, K.T., Čufar, K., 2013. Phenological variation in xylem and phloem formation in Fagus sylvatica from two contrasting sites. Agric. For. Meteorol. 180, 142–151. https://doi.org/10.1016/j.agrformet.2013.06.001.
R Core Team, 2022. R: A Language and Environment for Statistical Computing. R Foundation for Statistical Computing, Vienna, Austria. https://www.R-project.org/.
Rice, A., Glick, L., Abadi, S., Einhorn, M., Kopelman, N.M., Salman-Minkov, A., et al., 2015. The Chromosome Counts Database (CCDB) - a community resource of plant chromosome numbers. New Phytol. 206 (1), 19–26. https://doi.org/10.1111/nph.13191.
Richardson, A.D., O'Keefe, J., 2009. Phenological differences between understory and overstory. In: Noormets, A. (Ed.), Phenology of Ecosystem Processes: Applications in Global Change Research. Springer, Dordrecht, Heidelberg, pp. 87–117.
Rigo, D. de, Caudullo, G., Houston Durrant, T., San-Miguel-Ayanz, J., 2016. In: San-Miguel-Ayanz, J., Rigo, D. de, Caudullo, G., Houston Durrant, T., Mauri, A. (Eds.), The European Atlas of Forest Tree Species: Modelling, Data and Information on Forest Tree Species. European Atlas of Forest Tree Species. Publications Office of the European Union, Luxembourg pp. e01aa69+.
Roussel, J.-R., Auty, D., Coops, N.C., Tompalski, P., Goodbody, T.R., Meador, A.S., et al., 2020. lidR: an R package for analysis of Airborne Laser Scanning (ALS) data. Remote Sens. Environ. 251, 112061 https://doi.org/10.1016/j.rse.2020.112061.
Roussel, J.-R., Auty, D., Boissieu, F. de, Meador, A.S., Jean-Francois, B., Demetrios, G., et al., 2023. Package 'lidR'. https://cran.r-project.org/web/packages/lidR/index.html (accessed 07 November 2023).
Rudolf, H., 2023. Weltwald Freising. https://www.weltwald.de/fileadmin/user_upload/14-weltwald/pdfs/Weltwald_Freising_2023.pdf (accessed 27 September 2023).
Ryu, Y., Lee, G., Jeon, S., Song, Y., Kimm, H., 2014. Monitoring multi-layer canopy spring phenology of temperate deciduous and evergreen forests using low-cost spectral sensors. Remote Sens. Environ. 149, 227–238. https://doi.org/10.1016/j.rse.2014.04.015.
Schmeddes, J., Muffler, L., Barbeta, A., Beil, I., Bolte, A., Holm, S., et al., 2023. High phenotypic variation found within the offspring of each mother tree in Fagus sylvatica regardless of the environment or source population. Glob. Ecol. Biogeogr. https://doi.org/10.1111/geb.13794.
Schnablová, R., Huang, L., Klimešová, J., Šmarda, P., Herben, T., 2021. Inflorescence preformation prior to winter: a surprisingly widespread strategy that drives phenology of temperate perennial herbs. New Phytol. 229 (1), 620–630. https://doi.org/10.1111/nph.16880.
Schneider, U., Becker, A., Finger, P., Meyer-Christoffer, A., Rudolf, B., Ziese, M., 2011. GPCC Full Data Reanalysis Version 6.0 at 0.5: Monthly Land-Surface Precipitation From Rain-Gauges Built on GTS-based and Historic Data.
Schrodt, F., Kattge, J., Shan, H., Fazayeli, F., Joswig, J., Banerjee, A., et al., 2015. BHPMF - a hierarchical Bayesian approach to gap-filling and trait prediction for macroecology and functional biogeography. Glob. Ecol. Biogeogr. 24 (12), 1510–1521. https://doi.org/10.1111/geb.12335.
Segrestin, J., Navas, M.-L., Garnier, E., 2020. Reproductive phenology as a dimension of the phenotypic space in 139 plant species from the Mediterranean. New Phytol. 225 (2), 740–753. https://doi.org/10.1111/nph.16165.
Sporbert, M., Jakubka, D., Bucher, S.F., Hensen, I., Freiberg, M., Heubach, K., et al., 2022. Functional traits influence patterns in vegetative and reproductive plant phenology - a multi-botanical garden study. New Phytol. 235 (6), 2199–2210. https://doi.org/10.1111/nph.18345.
State Office for Digitization, Broadband and Surveying, 2023. BayernAtlas. https://geoportal.bayern.de/bayernatlas/?lang=de&topic=ba&bgLayer=atkis&catalogNodes=11&E=697066.10&N=5365947.32&zoom=11&layers=tk_by (accessed 02 November 2023).
Sun, S., Frelich, L.E., 2011. Flowering phenology and height growth pattern are associated with maximum plant height, relative growth rate and stem tissue mass density in herbaceous grassland species. J. Ecol. 99 (4), 991–1000. https://doi.org/10.1111/j.1365-2745.2011.01830.x.
Sun, S., Jin, D., Li, R., 2006. Leaf emergence in relation to leaf traits in temperate woody species in East-Chinese Quercus fabri forests. Acta Oecol. 30 (2), 212–222. https://doi.org/10.1016/j.actao.2006.04.001.
Tang, J., Körner, C., Muraoka, H., Piao, S., Shen, M., Thackeray, S.J., et al., 2016. Emerging opportunities and challenges in phenology: a review. Ecosphere 7 (8). https://doi.org/10.1002/ecs2.1436.
Toreti, A., Bavera, D., Acosta Navarro, J., Cammalleri, C., Jager, A. de, Di Ciollo, C., et al., 2022. Drought in Europe August 2022. Publications Office of the European Union, Luxembourg.
Uphus, L., Lüpke, M., Yuan, Y., Benjamin, C., Englmeier, J., Fricke, U., et al., 2021. Climate effects on vertical forest phenology of Fagus sylvatica L., sensed by Sentinel-2, time lapse camera, and visual ground observations. Remote Sens. 13 (19), 3982. https://doi.org/10.3390/rs13193982.
Vile, D., Shipley, B., Garnier, E., 2006. A structural equation model to integrate changes in functional strategies during old-field succession. Ecology 87 (2), 504–517. https://doi.org/10.1890/05-0822.
Violle, C., Choler, P., Borgy, B., Garnier, E., Amiaud, B., Debarros, G., et al., 2015. Vegetation ecology meets ecosystem science: permanent grasslands as a functional biogeography case study. Sci. Total Environ. 534, 43–51. https://doi.org/10.1016/j.scitotenv.2015.03.141.
Vitasse, Y., 2013. Ontogenic changes rather than difference in temperature cause understory trees to leaf out earlier. New Phytol. 198 (1), 149–155. https://doi.org/10.1111/nph.12130.
Vitasse, Y., Hoch, G., Randin, C.F., Lenz, A., Kollas, C., Scheepens, J.F., et al., 2013. Elevational adaptation and plasticity in seedling phenology of temperate deciduous tree species. Oecologia 171 (3), 663–678. https://doi.org/10.1007/s00442-012-2580-9.
Vitasse, Y., Lenz, A., Körner, C., 2014. The interaction between freezing tolerance and phenology in temperate deciduous trees. Front. Plant Sci. 5, 541. https://doi.org/10.3389/fpls.2014.00541.
Vitasse, Y., Baumgarten, F., Zohner, C.M., Rutishauser, T., Pietragalla, B., Gehrig, R., et al., 2022. The great acceleration of plant phenological shifts. Nat. Clim. Chang. 12 (4), 300–302. https://doi.org/10.1038/s41558-022-01283-y.
Walde, M.G., Wu, Z., Fox, T., Baumgarten, F., Fu, Y.H., Wang, S., Vitasse, Y., 2022. Higher spring phenological sensitivity to forcing temperatures of Asian compared to European tree species under low and high pre-chilling conditions. Front. For. Glob. Chang. 5, 1063127 https://doi.org/10.3389/ffgc.2022.1063127.
Wesołowski, T., Rowiński, P., 2006. Timing of bud burst and tree-leaf development in a multispecies temperate forest. For. Ecol. Manag. 237 (1–3), 387–393. https://doi.org/10.1016/j.foreco.2006.09.061.
Wu, S., Wang, J., Yan, Z., Song, G., Chen, Y., Ma, Q., et al., 2021. Monitoring tree-crown scale autumn leaf phenology in a temperate forest with an integration of PlanetScope and drone remote sensing observations. ISPRS J. Photogramm. Remote Sens. 171, 36–48. https://doi.org/10.1016/j.isprsjprs.2020.10.017.
Zani, D., Crowther, T.W., Mo, L., Renner, S.S., Zohner, C.M., 2020. Increased growing-season productivity drives earlier autumn leaf senescence in temperate trees. Science (New York, N.Y.) 370 (6520), 1066–1071. https://doi.org/10.1126/science.abd8911.
Zeng, L., Wardlow, B.D., Xiang, D., Hu, S., Li, D., 2020. A review of vegetation phenological metrics extraction using time-series, multispectral satellite data. Remote Sens. Environ. 237, 111511 https://doi.org/10.1016/j.rse.2019.111511.
Zohner, C.M., Renner, S.S., 2017. Innately shorter vegetation periods in North American species explain native-non-native phenological asymmetries. Nat. Ecol. Evol. 1 (11), 1655–1660. https://doi.org/10.1038/s41559-017-0307-3.
Zohner, C.M., Benito, B.M., Fridley, J.D., Svenning, J.-C., Renner, S.S., 2017. Spring predictability explains different leaf-out strategies in the woody floras of North America, Europe and East Asia. Ecol. Lett. 20 (4), 452–460. https://doi.org/10.1111/ele.12746.
Zohner, C.M., Mirzagholi, L., Renner, S.S., Mo, L., Rebindaine, D., Bucher, R., et al., 2023. Effect of climate warming on the timing of autumn leaf senescence reverses after the summer solstice. Science (New York, N.Y.) 381 (6653), eadf5098. https://doi.org/10.1126/science.adf5098.